Corrosion Science 53 (2011) 1873–1879

Contents lists available at ScienceDirect

Corrosion Science

journal homepage: www.elsevier.com/locate/corsci

Evaluation of cavitation erosion–corrosion degradation of mild steel by means of dynamic impedance spectroscopy in galvanostatic mode

J. Ryl *, K. Darowicki, P. Slepski

Department of Electrochemistry, Corrosion and Materials Engineering, Gdańsk University of Technology, Narutowicza 11/12, 80-952 Gdańsk, Poland

ARTICLE INFO

Article history:
Received 11 October 2010
Accepted 3 February 2011

Keywords:
A. Mild steel
B. EIS
B. Erosion

ABSTRACT

Cavitation erosion and corrosion of mild steel was studied by means of a vibratory facility in 3% w/w NaCl solution. Dynamic Electrochemical Impedance Spectroscopy (DEIS) measurements were carried out in the galvanostatic mode to allow on-line monitoring of impedance parameters in cavitation failure. The results, based on an analysis of instantaneous impedance spectra, correspond to degradation under the influence of cavitation erosion–corrosion. It has been shown that a change of pseudo-capacitance corresponds to an increase in sample roughness, while the charge-transfer resistance determines changes in the corrosion rate under the combined mechanical and electrochemical factors.

1. Introduction

Degradation due to cavitation is a complex phenomenon, that involves the joint interaction of mechanical and chemical factors in a hydrodynamic environment [1,2] and which should be considered as a unique type of material damage. In corrosive media, cavitation erosion degradation is connected with simultaneous corrosion of the material. In such situations, total degradation may exceed the sum of corrosion and erosion impact due to the presence of the synergistic effect of both factors [3]. Cavitation erosion has the effect of mechanically stripping off the corrosion film by the cavitation bubble collapse. Once the film has been removed, fresh reactive corrosion sites are generated depending on the repassivation rate and the integrity of the film. Other factors also influence corrosion-enhanced erosion: increase in mass transport caused by the high turbulence of the solution or decrease in the fatigue strength by corrosion effects. Erosion-enhanced corrosion takes place in the case of local corrosion at grain boundaries or removal of the hardened surface to expose the underlying base metal.

In general, the nature of the interaction is determined by a number of factors like passivity of the metal surface, adherence of the corrosion products, metallurgical state, diffusion of dissolved oxygen, presence of aggressive ions and the intensity of cavitation [2,4–6]. For instance, in 3% w/w sodium chloride solution, the fractional weight loss of cast iron due to pure corrosion ranges from 1% to 10%, while weight loss due to corrosion-induced erosion can range as high as 90% [7]. For copper and its alloys in seawater, synergism ranging to 50% of the overall material loss was determined in the presence of mild corrosion [8].

In erosion processes, it is clear that material removal occurs by mechanical means as a consequence of cavity collapse [2]. This can be enhanced by chemical and electrochemical factors. Few techniques have been used to study corrosion under cavitation conditions, but its mechanism is not yet fully understood. The basic tool for the evaluation of cavitation erosion resistance as well as the synergistic influence of corrosion on the degradation rate is a function of weight loss [3,9,10], combined with the corrosion potential and polarisation curves. Engelberg and Yahalom [11] obtained polarization curves of steel specimens eroded in an ultrasonic vibratory cavitation device. Kwok et al. [5] investigated synergistic effect of cavitation erosion and corrosion of various engineering alloys in 3.5% w/w NaCl solution. In their studies, exposure of most investigated materials to cavitation shifts the free corrosion potential towards more negative values; however, in the case of mild steel, cavitation exposure induced a shift of free corrosion potential by approx. 150 mV in the positive direction. Authors couple this effect with the corrosion film or product detachment and increase in mass transport under the generation of ultrasound. This positive shift of potential in the case of mild steels might be a reason of its low corrosion resistance.

Luo et al. and Jiang et al. [6,11] carried out Electrochemical Impedance Spectroscopy (EIS) measurements of low-alloy steel in different solutions to elucidate the corrosion mechanism under cavitation conditions. The free corrosion potential was shifted to higher positive values and the registered data showed the diminished impedance values during cavitation exposure. However, within the time required to obtain a single impedance spectrum, corrosion resistance of material and its surface roughness changed

* Corresponding author. Tel./fax: +48 583471092.
E-mail address: jacekr@chem.pg.gda.pl (J. Ryl).

0010-938X/$ - see front matter © 2011 Elsevier Ltd. All rights reserved.
doi:10.1016/j.corsci.2011.02.004

significantly, which may lead to sample polarisation. Thus, the traditional approach of EIS is limited in such systems.

Precise determination of the dynamics of changes to electrochemical parameters under cavitation exposure plays a key role to understand the synergistic mechanism and minimisation of degradation caused by corrosive factors. Dynamic Electrochemical Impedance Spectroscopy (DEIS) proposed by Darowicki [13] offers an alternative approach. Some of its theoretical background can be found later in the manuscript. DEIS overcomes the problem of non-stationary conditions [14–16]. Ryl and Darowicki [16] have carried out DEIS electrochemical monitoring of cavitation erosion of carbon steel under the influence of corrosive factors. It was proven that cavitation erosion–corrosion has an influence on the impedance parameters, which depends on the excitation energy of the ultrasonic wave. Evaluation of the qualitative information of corrosion factors influencing the erosion–corrosion were presented and discussed.

Under the influence of erosion–corrosion, the free corrosion potential is shifted. Forcing the constant values of the potential during the experiment leads to the generation of polarisation currents, which do not occur in real conditions. This situation took place in the previous work of the authors [17], where the sample potential was fixed in the quiescence state. Measurements in the galvanostatic mode with the resultant current equal to zero can help examine the behaviour of a freely corroding sample under cavitation influence without any polarisation influence. The concept of modifications of EIS measurements in the galvanostatic mode is not novel and can be found in the literature [18,19]. This paper presents possible applications of DEIS measurements in a three-electrode system in the galvanostatic mode as a tool to monitor the cavitation erosion–corrosion process.

2. Dynamic Electrochemical Impedance Spectroscopy

The EIS technique relies on three cardinal conditions: linearity, causality and stationarity, which need to be fulfilled in order to achieve valuable experimental data. The latter condition is the most difficult to achieve because the majority of the electrochemical processes are naturally non-stationary. In classical EIS, the investigated systems are excited step by step with perturbation signals of different frequencies. The principal disadvantage of such an approach is the length of measurement, which can be given as (1):

$$t = \sum_{i=1}^{k} \frac{n}{f_i} \tag{1}$$

where: t, total time of excitation; f_i, consecutive frequencies of perturbation signal; n, number of periods for each frequency.

Dynamic Electrochemical Impedance Spectroscopy (DEIS) is an alternative approach that is based on simultaneous excitation of system with all perturbation frequencies. A resultant perturbation signal I_{ac} is a composition of current sinusoids, each of them described by their own amplitude i_j, frequency ω_j and phase shift ψ_j as presented in Fig. 1 (j = 1,2, . . ., k). In the case of random distribution of phase shifts, as it is in pseudo-white noise local synchronisation of components, the maxima are possible. This effect is unfavourable for the measurement since the resultant peak-to-peak amplitude increases and the system might be brought out of a steady state [20]. The selection and composition of adequate amplitudes and phase angles is made with an application written in LabView environment for this purpose. The perturbation signal is subsequently composed with galvanostatic signal.

The proper selection of sampling frequency is very important. According to the Nyquist criterion, the signal must be sampled at least twice as high as its highest frequency in order to extract all of the information from the bandwidth and accurately represent the potential response signal [21]. On the other hand, a very high sampling frequency can exceed the hardware capabilities. In the case of perturbation, the signal is composed of frequencies ranging up to 45 kHz and the sampling frequency was set up to be 125 kHz.

The acquired signals must be transformed to give the resultant amplitudes and phase angles. Fourier and Laplace transformations are popular; however, they don't provide time localisation. For experiments carried out in dynamic conditions, allocation of the impedance data acquired for the instantaneous state of the system is problematic. Short-time Fourier transformation (STFT) overcomes this problem [22,23]. However, to obtain the impedance spectra change over time, one must use the decomposition process of windows with a finite length, which are acquired with the use of Short-time discrete Fourier transformation (STDFT) [24]. The window length is chosen on the basis of the perturbation signal

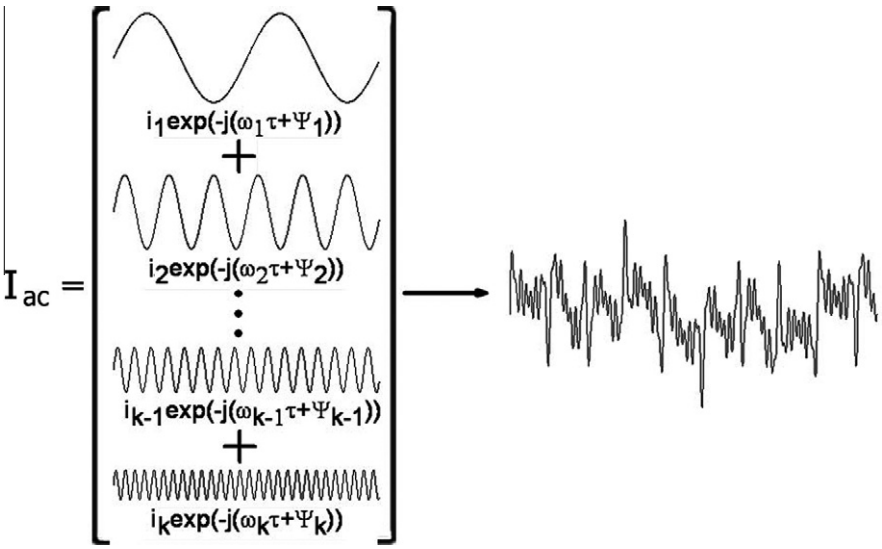

Fig. 1. Schematic composition of the perturbation signal.

Table 1
Chemical constitution of investigated alloy in wt.%.

Fe	Si	C	Cu	Mn	Ni	Cr
Bal.	0.35	0.22	0.3	1.1	0.3	0.3

composition. It must be long enough to contain at least a few periods of the lowest frequency component and short enough to confirm the assumption of the system pseudo-stationarity. This window cuts fragments of the registered signal and transforms them with the appropriate window function. Repeating the sequence of cutting, STDFT application allows to obtain the series of impedance spectra in the time domain [14,25].

In order to obtain a pseudo-stationary measurement, a narrow window is necessary, the length of which determines the lowest frequency of the perturbation signal. For this reason, one of the main drawbacks of DEIS technique is that the measurements are limited to the low-frequency range. The more stationary the process is, the lower frequencies can be used (but a longer analysing window is required). This technique is averaging of the Fourier spectra. But, it averages only the window length. Hence, we are able to obtain valid instantaneous impedance spectra even if the whole investigated process is non-stationary. Detailed information regarding DEIS measurements carried out in the galvanostatic mode was presented by Slepski et al. [26].

3. Experimental

Cavitation was induced with a vibratory facility, which takes high-frequency oscillations of the piezoelectric transducer, to generate pressure fluctuations with its tip immersed in the solution. These fluctuations are sufficient for generation and further implosion of cavitation bubbles. The piezoelectric transducer was vibrating at a frequency of 20 kHz with a peak-to-peak amplitude equal to 30 μm. Vibratory apparatus is standardised according to ASTM G32 [27] and is the most commonly used method of cavitation generation in laboratory conditions.

Measurements were carried out with a three-electrode system in 3% w/w NaCl. The working electrode was carbon steel (its constitution is presented in Table 1). Prior to each experiment, samples were ground with 500–1600 grade emery papers and mounted 1 mm below the tip of the ultrasound transducer. The surface area exposed to cavitation erosion–corrosion was 1.16 cm^2. The reference electrode was Ag/AgCl, the concentration of chloride ions was 0.508 mol/dm^3 and the standard potential +0.25 V vs. SHE. The counter electrode was platinum mesh.

The perturbation signal was a package composed of 20 elementary current sinusoids lying in the frequency range from 45 kHz to 7 Hz. Perturbation amplitudes were selected in such a way to assure that the resultant response signal peak-to-peak amplitude would not exceed 10 mV at any stage of experiment. The size of the analysing window was equal to 1s, which means that each impedance spectra represents an averaged impedance value from this time period. The sampling frequency was equal to 125 kHz.

The sample was held 1 mm below the tip of the transducer. In order to avoid interferences of the piezoelectric vibration generator with an AC measurement, the tip was made of polyetheretherketone (PEEK) with a very high resistance to the cavitation erosion while providing electric insulation between the 20 kHz generator and the electrochemical system. After the single measurement, the tip was replaced. The authors have carried out the Kramers–Kronig signal analysis in order to detect the effect of the 20 kHz frequency on the response signal. For each perturbation frequency, the relative contribution of the 2nd and 3rd harmonics does not exceed 0.4% of the primary component during the impedance data acquisition.

The experiment had a cyclic character; the cycles were composed of a cavitation exposure period, t_i = 30 s (i = 1,2,. . .,n), and the cavitation quiescence period. The single cycle was T_i = 120 s. Fig. 2 represents the scheme of the current/potential response signal changes under cavitation/quiescence cycles. Instantaneous impedance data were taken for the entire period of the experiment; however, impedance spectra were analysed only at one point, c_i, a second before turning off the cavitation exposition. Impedance data is presented as a function of the cavitation exposure time t_{cav}.

After each experiment, samples were placed in the ultrasonic cleaner to detach any loose material, dried and weighted. SEM micrographs were taken for each sample after 20, 60 and 120 min of the cavitation erosion–corrosion exposure.

4. Results and discussion

In Fig. 3, one can see changes to the potential, which result from cavitation exposure of the investigated mild steel sample in the galvanostatic mode under zero current conditions. A sudden shift of the potential of around 200 mV to more positive values is a typical behaviour under the influence of the vibratory cavitation

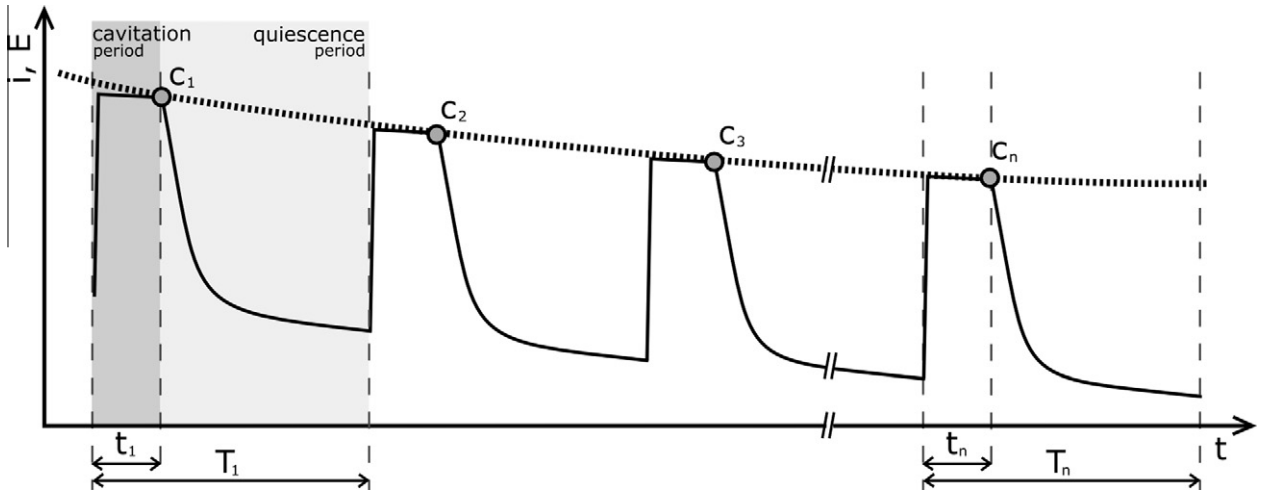

Fig. 2. Schematic representation of data used for DEIS analysis as a function of t_{cav}.

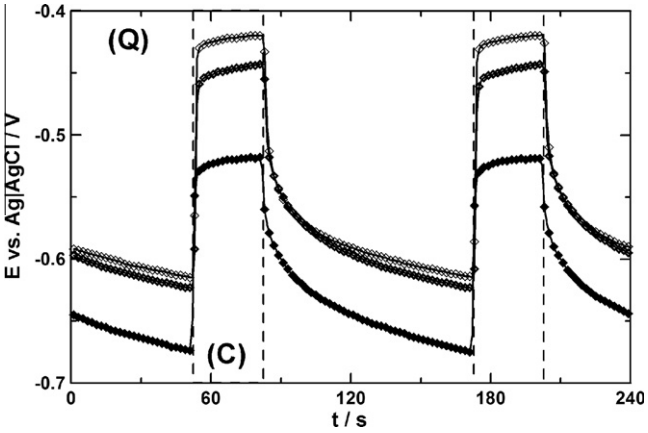

Fig. 3a. Changes of potential registered under zero current conditions applied from the galvanostat. The quiescence phase (*Q*) and cavitation exposure phase (*C*) after 20 min (◇), after 40 min (◆), after 100 min (◆) of cavitation exposure.

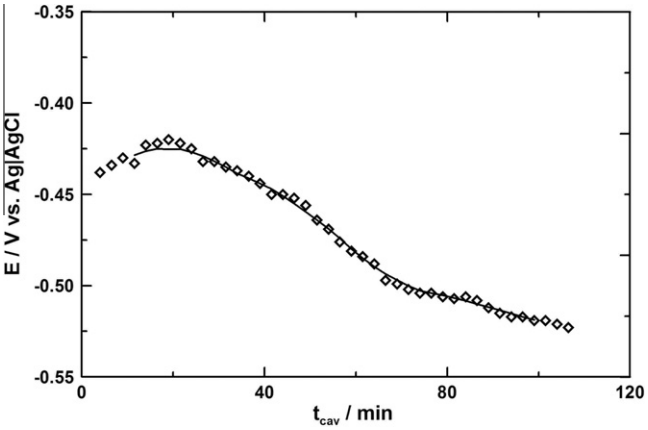

Fig. 3b. Changes of the open circuit potential for 2 h of cavitation exposure.

generator, although its value depends on the investigated material and solution [2,4,5,17]. Such shifts are recurrent with each cycle and are most likely caused by an increase in mass transport, that is induced by the transducer vibrations, as well as by formation and collapse of cavitation bubbles. They might also be attributed to the degradation of a thin layer of corrosion products on the sample surface. During the measurement, the potential becomes more negative regardless of the cavitation/quiescence phase (Fig. 3b).

A decrease in the electrode potential measured in the galvanostatic mode with the resultant current equal to zero (the working counter electrode should be connected primarily to the state of the surface. Such behaviour, i.e. decrease in the corrosion potential, is characteristic of most corroding systems. Development of the sample surface resulting from an increase in the roughness under cavitation erosion intensifies the corrosion degradation of the material. Also, the solution temperature increases the corrosion rate. Outer cooling and the large volume of thee experimental cell lead to smaller changes to the temperature; however, complete elimination of heating is impossible.

It was observed that the solution progressively changed colour to brown when the sample is exposed to cavitation erosion–corrosion, and black deposits were visible on the sample surface. The authors suggest that this is due to iron corrosion. For low oxygenated solutions, reactions leading to Fe_3O_4 formation take place. These oxides are black and are characterised by good adhesion to the steel surface as seen in this case. Other forms of hydroxides and oxides are usually formed in the upper part of the corrosion product layer and are transported to the solution as a result of ultrasonic vibrations and implosion of cavitation bubbles that colour it with a brown shade. Similar observations were done by Kwok on steels and cast irons undergoing cavitation attack in 3.5% w/w NaCl [4].

Fig. 4 presents SEM micrographs of investigated mild steel samples taken after 20 min (Fig. 4a), 60 min (Fig. 4b) and 120 min (Fig. 4c) of cavitation exposure. After 20 min of the measurement, the sample surface is still uniform. Scratches from mechanical grinding with abrasive paper are visible, locally deformed with tensions arising during implosion of the cavitation bubbles. A few cavities are present, each of them is less than 10 μm in diameter and is very shallow. The pulsatory applied stresses promote the accumulation of fatigue-like hardening in metals, even if the stresses are less than the yield stress [2]. After the incubation period is over, the material starts to deform and whole grains detach. In Fig. 4b, one can see a large number of pits arising due to mechanical erosion, assisted by corrosion processes which greatly increase the surface roughness. Constant influence of cavitation erosion leads to further material detachment and further pit generation (Fig. 4c).

Fig. 5 illustrates the discrete changes of impedance spectra as a function of cavitation time $t_{cav.}$ Impedance spectra and resistance of the electrolyte diminish over time. This effect is most evident for the first 40 min of the experiment. Moreover, the shape of impedance spectra changes with the time of cavitation exposure. In the early phase of measurements, a small loop was visible in the Nyquist plot for the very high frequency range (Fig. 6a). This loop vanishes after the incubation period. Sfaira et al. [28] suggested its relation with the existence of a very thin layer of insoluble corrosion products on the sample surface.

To accommodate the equivalent electrical circuit, a model containing two time constants R(C(R(QR))) was taken into consideration, with the high frequency time constant representing the resistance and capacitance of surface layer. It should be noted that the resistance of the high frequency time constant is two orders of magnitude lower as compared to R_{ct} and might result in high errors during the determination of this parameter. After t_{cav} = 40 min, the resistance of the high frequency time constant drops to zero.

For both equivalent electrical circuits, the impedance data analysed manifest a similar tendency of changes with cavitation exposure. The two-time-constant equivalent electrical circuit is only effective for a short experimental period, after which it reveals a higher level of data scattering; therefore, a single-time-constant equivalent electrical circuit R(QR) was used for further analysis. This circuit was previously applied for the analysis of mild steel undergoing cavitation erosion in a sodium chloride solution [5,12,17]. The circuit consists of the solution resistance R_s, the constant phase element (CPE) and the parallel resistance R_{ct}, which corresponds to the charge transfer resistance. The impedance of CPE is given by equation (2).

$$Z_{CPE} = [Q(j\omega)^n]^{-1} \quad (2)$$

For *n* equal to one, Eq. (2) represents the impedance of a capacitor. Lower values of n between 0.7 and 0.9 are often obtained with solid electrodes in aqueous solutions in the audio and sub-audio frequency range. Much lower values of around 0.5 have frequently been observed with porous electrodes. The rougher the surface, the larger the deviation from the ideal capacitive behaviour is. Therefore, the CPE might be a good tool to evaluate the sample surface roughness and heterogeneity [29–31].

The solution resistance R_s was equal to 8 Ωcm^2 at the beginning of incubation period and decreased to around 6 Ωcm^2 at the end of incubation period. As a result of cavitation degradation the, sample

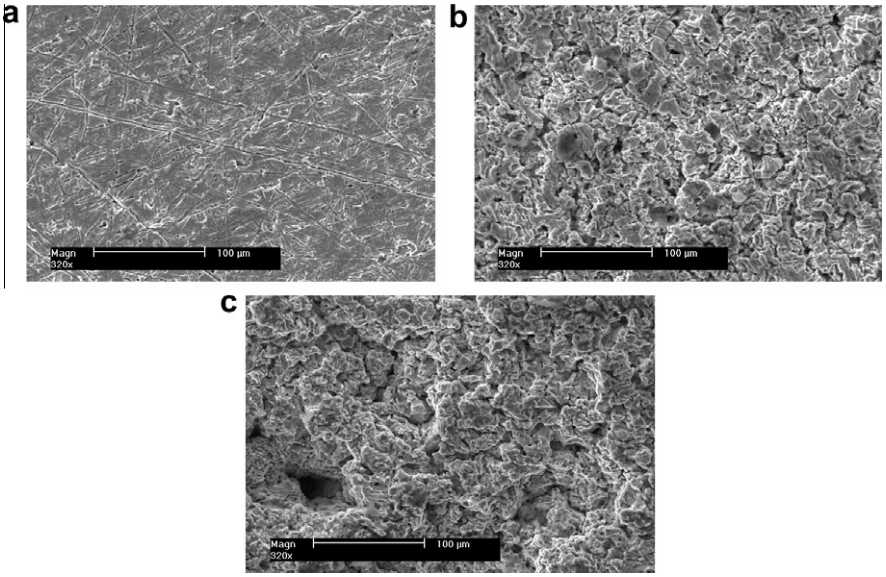

Fig. 4. SEM micrographs taken after (a) 20 min, (b) 60 min and (c) 120 min of cavitation exposure of mild steel sample in 3% w/w NaCl.

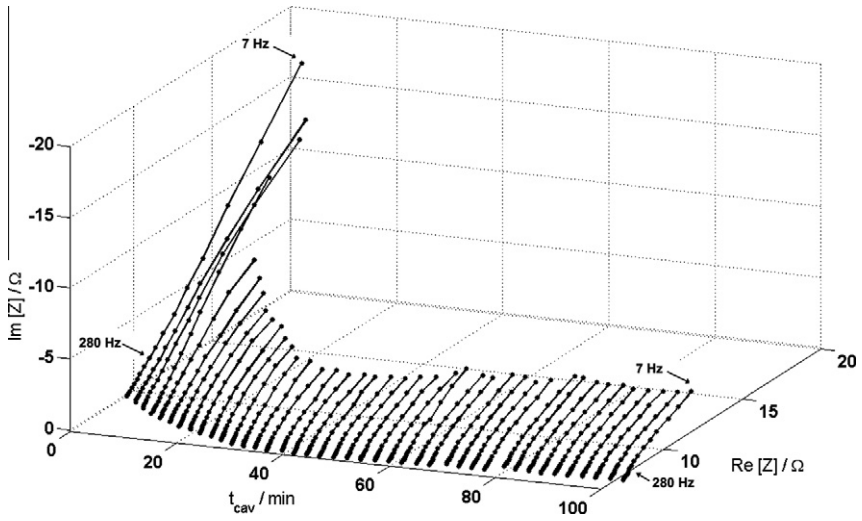

Fig. 5. 3D representation of impedance changes with cavitation exposure time plotted on a *z*-axis for mild steel sample immersed in 3% w/w NaCl solution presented in a form of Nyquist plot.

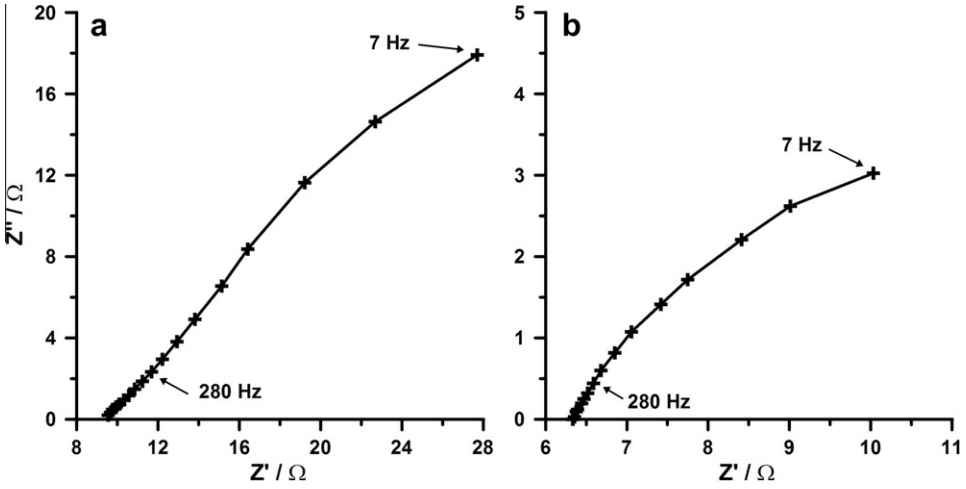

Fig. 6. Nyquist plot for (a) t_{cav} = 5 min and (b) t_{cav} = 80 min of the cavitation exposure of mild steel sample in 3% w/w NaCl solution.

material goes into the solution due to chemical dissolution or mechanical erosion, leading to a decrease in solution resistance.

The CPE behaviour is generally attributed to surface roughness or fractal geometry, electrode porosity and inhomogeneity [32–34]. The qualitative changes of the Q parameter evolution as a function of time depend mostly on changes in the surface area as a result of an increase in the surface roughness. The changes of the Q parameter during 2 h of measurement are presented in Fig. 7a. During the first 40 min of experiment, only small changes are visible. Afterwards, the Q parameter highly increases. Fluctuations of the measurement points, especially for later exposure times, is a consequence of the high dynamics of the system.

The Q parameter should be connected to the mechanical changes of the sample surface roughness. During the initial stage, material detachment is negligible as stresses arising from implosion of cavitation bubbles accumulate in material, but do not lead to erosion and the value of $Q(t)$ is constant. The incubation period was estimated to last for around 40 min as based on the SEM micrographs and changes of CPE. Once the critical point is reached, the material starts to mechanically detach, the surface area increases and as a consequence, the Q parameter increases. Further drop of $\Delta Q/\Delta t_{cav}$ ratio might be connected to the cushioning effect held by an insoluble, highly adhesive layer of corrosion products; this, however, requires further research. Also, the n parameter presented on Fig. 8 decreases over time, which is connected to an increase in the surface roughness.

The impedance measurements carried out for reference purposes under steady corrosion (without cavitation) indicate that the Q parameter is about two orders of magnitude lower than when exposed to cavitation. This parameter is associated with

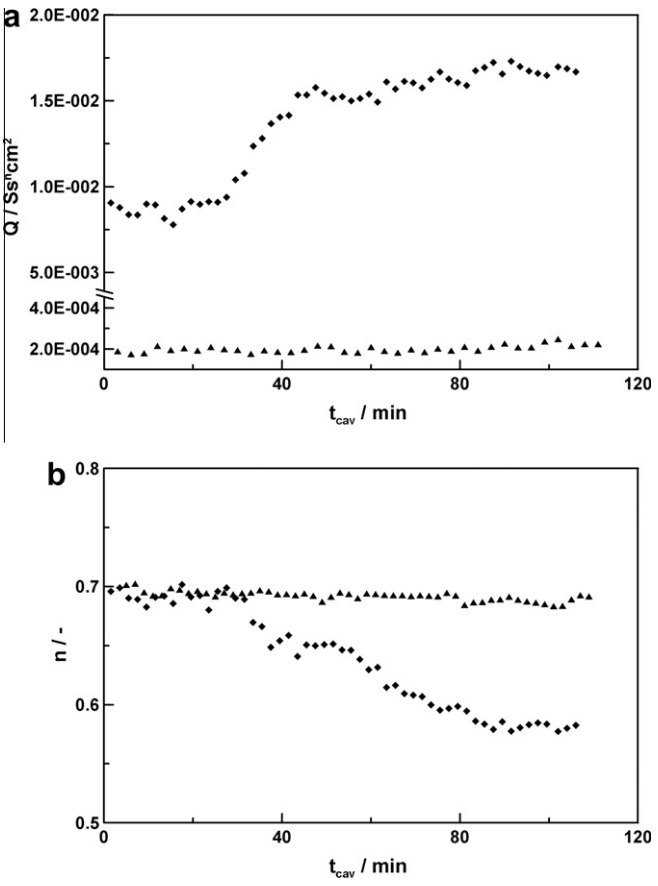

Fig. 7. Changes to the CPE parameters, Q and n, under cavitation exposure (◆) and under steady corrosion conditions (▲) as estimated by means of R(QR), the electric equivalent circuit.

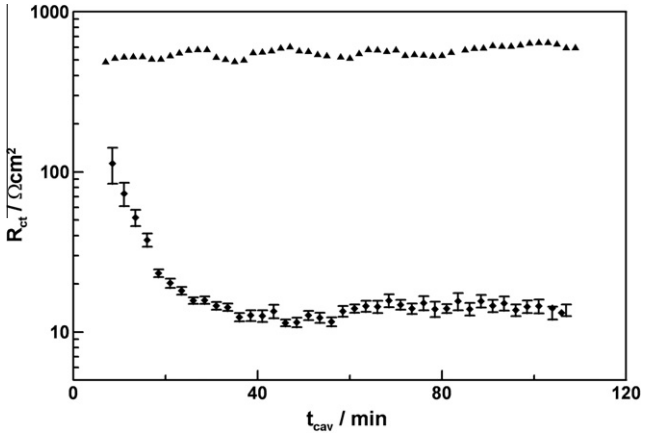

Fig. 8. Changes to the R_{ct} parameter under cavitation exposure (◆) and under steady corrosion conditions (▲), as estimated by means of R(QR), the electric equivalent circuit.

the electric double layer capacitance; therefore, it is most likely that the difference results from changes in the vicinity of the electrode, which are induced by ultrasound generator. As the reference sample does not undergo cavitation erosion, there is no noticeable increase in the Q parameter as a result of the surface development. Similarly, the n parameter presented in Fig. 7b decreases over time under cavitation erosion–corrosion exposure, which is connected to an increase in the surface roughness. Exposure to corrosive agents without cavitation presence is accompanied by imperceptibly small, linear changes of the n parameter.

The charge transfer resistance, R_{ct}, decreases during the incubation period (Fig. 8) as an effect of the synergistic corrosion and erosion degradation of the investigated sample. The highest R_{ct} drop appears during the incubation period and precedes visible mechanical degradation of the sample as represented by CPE. During this period, a black layer of corrosion products with good adhesion and partial solubility in the solution is formed. This layer of corrosion products is non-uniform, allowing free charge transfer between the sample and the solution.

During implosion of cavitation bubbles, two competing processes of tension transfer to the adjacent material surface can be distinguished: the acoustic wave and liquid jet penetrating the cavitation bubble during its collapse [2]. The presence of the growing insoluble layer of corrosion products due to less corrosion processes has a direct influence on the subsequent cavitation erosion resistance of the material. It creates a cushioning effect for the collapsing cavitation bubble that absorbs part of the energy resulting from the implosion. Decrease in the degradation rate due to the presence of corrosion product layer is one of the synergistic interactions between erosion and corrosion. After the surface is fully covered with the corrosion product layer, the R_{ct} resistance remains constant with an average value of 18 Ωcm^2.

Electrochemical corrosion corresponds mainly to the charge transfer resistance and diffusion transport of the reagent to the electrode surface. The charge transfer resistance is shown in most cases for frequencies above 1 Hz. For the lower frequencies, the diffusion transport process is dominant. In order to obtain impedance spectra containing the diffusion processes, it is necessary to use a perturbation signal with frequencies far below 1 Hz, which is a limitation to the DEIS technique as presented in this case. However, the ultrasound creates a hydrodynamically modulated mass transport in electrochemical experiments. This modulation appears to arise from the combined effects of acoustic cavitation and the field-induced fluid motion driven at a frequency of the ultrasound [35]. Diffusion transport of the reagent can be neglected because of stirring at high ultrasonic frequencies during

the vibratory cavitation exposure. It remains difficult to estimate R_{ct} value by means of DEIS during the cavitation quiescence phase (with the use of the same perturbation signal frequency range and the analysing window). On the basis of the measurements carried out for the frequency range, including very low frequencies down to 10 mHz, the authors estimated R_{ct} to be two orders of magnitude higher during the quiescence phase than while under cavitation exposure. Such a difference in the R_{ct} value is related to the increased mass transport under the influence of ultrasound. Loss of corrosion resistance may be also connected with partial removal of the corrosion product layer from the surface, thus exhibiting the bare reactive metal.

5. Conclusions

The Dynamic Electrochemical Impedance Spectroscopy technique in the galvanostatic mode was used as a tool for observing the changes of electrochemical parameters while submitting mild steel samples to cavitation erosion. Obtaining instantaneous impedance spectra allowed the determination of changes to the electric circuit parameters of the system under cyclic cavitation exposure.

CPE parameters: Q and n changes were bounded mostly to the mechanical erosion of material surface, which leads to an increase in surface roughness. Their changes are not significant during the incubation period, in which material detachment under cavitation erosion is negligible. R_{ct} parameters help determine corrosion resistance changes that result from cavitation exposure. It is highly diminished during the incubation period, resulting in a growth consisting of a layer of black products of corrosion.

Acknowledgements

This research was supported by a grant financed by the Polish Ministry of Education and Science, N N507 4476 33. This research was supported by the European Union within the European Social Fund within the framework of the project "InnoDoktorant – Scholarships for PhD students, 1st edition".

References

[1] R.J.K. Wood, J.A. Wharton, A.J. Speyer, K.S. Tan, Tribol. Int. 35 (2002) 631–641.
[2] C.T. Kwok, F.T. Cheng, H.C. Man, Mat. Sci. Eng. A290 (2000) 55–73.
[3] ASTM G119-93, ASTM, Philadelphia, PA.
[4] A. Karimi, J.L. Martin, International Metals Reviews 31 (1986) 1–26.
[5] C.T. Kwok, F.T. Cheng, H.C. Man, Mat. Sci. Eng. A290 (2000) 145–154.
[6] S.Z. Luo, Y.G. Zheng, M.C. Li, Z.M. Yao, W. Ke, Corrosion 59 (2003) 597–605.
[7] Z. Xiaojun, L.A. Procopiak, N.C. Souza, A.S.C. M d'Oliveira, Mat. Sci. Eng. A 358 (2003) 199–204.
[8] W.J. Tomlinson, M.G. Talks, Tribol. Int. 24 (1991) 67–75.
[9] R.J.K. Wood, S.A. Fry, J. Fluids Eng. 111 (1989) 271–276.
[10] G. Engelberg, J. Yahalom, Corros. Sci. 12 (1972) 469–473.
[11] S.L. Jiang, Y.G. Zheng, Z.M. Yao, Corros. Sci. 48 (2006) 2614–2632.
[12] K. Darowicki, J. Electroanal. Chem. 486 (2000) 101–105.
[13] K. Darowicki, J. Kawula, Electrochim. Acta 49 (2004) 4829–4839.
[14] S. Krakowiak, K. Darowicki, P. Slepski, J. Electroanal. Chem. 575 (2005) 33–38.
[15] G.A. Ragoisha, A.S. Bondarenko, Electrochim. Acta 50 (2005) 1553–1563.
[16] J. Ryl, K. Darowicki, J. Electrochem. Soc. 155 (2008) P44–P49.
[17] P.T. Wojcik, M.E. Orazem, Corrosion 54 (1998) 289–298.
[18] P.T. Wojcik, P. Agarwal, M.E. Orazem, Electrochim. Acta 41 (1996) 977–983.
[19] ASTM G32-98, ASTM, Philadelphia, PA.
[20] P. Slepski, K. Darowicki, J. Electroanal. Chem. 633 (2009) 121–126.
[21] J. Hazi, D.M. Elton, W.A. Czerwinski, J. Schiewe, V.A. Vicente-Beckett, A.M. Bond, J. Electroanal. Chem. 437 (1997) 1–15.
[22] R.G. Lyons, Understanding Digital Signal Processing, Addison-Wesley/Longman, New York, 1997.
[23] L. Cohen, Time–Frequency Analysis, Prentice-Hall, Englewood Cliffs, NJ, 1995.
[24] L. Cohen, C. Lee, Instantaneous frequency, in: B. Boashash (Ed.), Time–Frequency Signal Analysis, Wiley Halsted Press, Lingman Cheshire, 1992.
[25] S. Qian, D. Chen, Joint Time–Frequency Analysis: Methods and Applications, Prentice-Hall PTR, Englewood Cliffs, NJ, 1996.
[26] K. Darowicki, P. Slepski, Journal of Electroanalytical Chemistry 547 (2003) 1–8.
[27] M. Sfaira, A. Srhiri, H. Takenouti, M. Marie de Ficquelmont-Loizos, A. Ben Bachir, M. Khalakhil, J. Appl. Electrochem. 31 (2001) 537–546.
[28] A. Lasia, Electrochemical Impedance Spectroscopy and its Applications, Modern Aspects of Electrochemistry, vol. 32, Springer, New York, 1999.
[29] Z. Yao, Z. Jiang, F. Wang, Electrochim. Acta 52 (2006) 4539–4546.
[30] J. Jorcin, M. Orazem, N. Pebere, B. Tribollet, Electrochim. Acta 51 (2006) 1473–1479.
[31] C.H. Kim, S.I. Pyun, J.H. Kim, Electrochim. Acta 48 (2003) 345–354.
[32] A. Lasia, J. Electroanal. Chem. 397 (1995) 27–33.
[33] T. Pajkossy, T. Wandlowski, D.M. Kolb, J. Electroanal. Chem. 414 (1996) 209–220.
[34] E.L. Cooper, L.A. Coury, J. Electrochem. Soc. 145 (1998) 1994–1999.
[35] C.G. Duan, V.Y. Karelin, Abrasive erosion and corrosion of hydraulic machinery, Imperial College Press, London, 2002.